IEEE Access
Multidisciplinary ⋮ Rapid Review ⋮ Open Access Journal

Received 17 May 2022, accepted 15 June 2022, date of publication 24 June 2022, date of current version 13 July 2022.

Digital Object Identifier 10.1109/ACCESS.2022.3185999

The Effect of Parasitic Patches Addition on Bandwidth Enhancement and Mutual Coupling in 2 × 2 Sub-Arrays

FITRI AMILLIA[1,2], (Student Member, IEEE), EKO SETIJADI[1], (Member, IEEE), AND GAMANTYO HENDRANTORO[1], (Senior Member, IEEE)

[1]Department of Electrical Engineering, Institut Teknologi Sepuluh Nopember, Surabaya 60111, Indonesia
[2]Department of Electrical Engineering, Universitas Islam Negeri Sultan Syarif Kasim Riau, Pekanbaru 28293, Indonesia

Corresponding author: Eko Setijadi (ekoset@ee.its.ac.id)

This work was supported in part by the Indonesian Ministry of Religions Affairs through the Ministry of Religions Affairs (MORA) 5000 Doctor Scholarship Program under Grant 2644/DJ.I/Dt.I.III/PP.04/08/2018; and in part by the Indonesian Ministry of Research, Technology and High Education through the Konsorsium Riset Unggulan Perguruan Tinggi (KRUPT) Research Grant 705/PKS/ITS/2019.

ABSTRACT This paper presents a 2 × 2 sub-array design with elements having parasitic patches (PPs) for massive MIMO applications. The frequency chosen for the design is 3.5 GHz, one of the 5G frequency allocations. A coaxial feeding probe is employed. For each sub-array element, multiple PPs are placed on the top layer to enhance the bandwidth. We show that with a greater number of PPs, the bandwidth of an element can be increased considerably with respect to previous designs. Two types of single element antenna with 5 and 10 PPs exhibit a bandwidth of more than 600 MHz and 700 MHz or a fractional bandwidth of about 17% and 20%, respectively. The increase in element dimension and, consequently, element spacings reduces the mutual coupling in the sub-array. Simulation results and measurements of the 2 × 2 sub-arrays with the 5-PP and the 10-PP elements show that the sub-arrays meet the desired performance with return loss less than −10 dB and bandwidth of 567 MHz and 730 MHz, respectively. Mutual coupling effects can be suppressed to less than −20 dB in the frequency range of 3.202 GHz − 3.934 GHz.

INDEX TERMS Antenna, sub-array, massive MIMO, bandwidth, mutual coupling, parasitic patch.

I. INTRODUCTION

Massive Multiple-Input Multiple-Output (M-MIMO) scheme is one of the key enabling technologies of 5G communications. M-MIMO uses a large number of antenna elements grouped into sub-arrays that work at the same time and frequency [1], [2]. Wide bandwidth is one of the key requirements in antenna design for 5G applications. Several techniques have been proposed to achieve it [3]. On the other hand, the requirement of having many antennas in M-MIMO demands a compact design to save on fabrication and installation. The challenge of designing a compact antenna is to make the spacing between elements smaller, which makes it practically impossible to avoid the mutual coupling effects [4], [5]. Such effects, among others, include the blindness to some directions of arrival [6], increasing error rate [7], and reduced capacity [8] of the M-MIMO communication system.

The associate editor coordinating the review of this manuscript and approving it for publication was Mohammed Bait-Suwailam.

However, it appears that simultaneously achieving wide bandwidth, compactness and low mutual coupling remains challenging.

Several studies to reduce mutual coupling have been conducted, but many of the proposed designs have resulted in the loss of compactness of the antenna dimensions, especially in microstrip array antennas, due to addition of relatively bulky structures integrated into the design that also causes difficulties and more expensive fabrication. Some of these methods include electromagnetic bandgap (EBG) isolator [9], [10], metasurface [11], coplanar wall [12], and stacked patches [13].

However, there are several methods that are effective in reducing mutual coupling without having to eliminate the compactness of the microstrip antenna with a few tolerable drawbacks, namely the defected ground structure (DGS) method [14], resonator [15], [16], a combination of DGS and line resonator [17] and parasitic patch technique [18].

While the techniques in [14]–[17] do not provide wide bandwidth, the parasitic patch technique is potential to achieve wideband characteristic. In this paper, we focus on the parasitic patch technique.

Reference [18] presents an antenna design consisting of layers of a substrate with 4 parasitic patches (PPs) placed on the top layer of the antenna, while the array application uses a combination of two decoupling techniques by arranging a 2×2 antenna. The combination of the two techniques used is decoupling walls and neutralized networks. The metal wall not only makes the above two parasitic patches short-circuited easily, but it also acts as a decoupling wall to reduce the adverse mutual coupling between the antenna elements. Furthermore, simple decoupling of short-circuit stepped impedance structures (SSISs) as a neutralizing network is added to reduce mutual coupling even further. The antenna is made up of two layers of substrate being 1.5 and 2 mm thick, respectively. All antenna structures are in a rectangular cavity formed by metal via as sidewalls. Here, two substrate layers are used to easily embed SSIS decoupling in array applications. This causes the antenna to be more costly for fabrication and less compact. The design achieves a frequency range of 3.35 to 3.95 GHz or a fractional bandwidth of 16%, a gain of 13.6 dB and mutual coupling below −38 dB.

In [19], the authors designed a sub-array of two rectangular antenna elements at a frequency of 2.8 GHz. Simulation results show that in the E field for all element spacings, the mutual coupling is less than −20 dB. However, the mutual coupling in the H plane for all element spacings is more than −20 dB. The bandwidth is 77.3 − 88.5 MHz with varying element spacing, which is still below 100 MHz and much below the required bandwidth for 5G applications. Subsequently, the authors of [20] report on the design of a two-element sub-array using 5 PPs placed on the top layer of the antenna and one substrate layer. The design is simulated and arranged in the H-plane for 0.75λ spacing resulting in mutual coupling of −29.76 dB and the E-plane of −33.56 dB. On the other hand, mutual coupling in the E-plane for 0.5λ spacing does not meet the maximum mutual coupling criterion. The fractional bandwidth is 17%, and the resulting bandwidth is 609.9 − 616.4 MHz for all variations of element spacing suitable for 5G applications.

This paper presents a simple yet effective strategy in dealing with the requirements of both the wide bandwidth and low mutual coupling. We present a 2×2 sub-array design with a parasitic patch technique for use in M-MIMO 5G applications. The frequency chosen by the author is 3.5 GHz, which is one of the sub-6 GHz carriers used for 5G applications. We show that the use of more PPs can lead to a sub-array with greater bandwidth. We extend the technique of adding parasitic patches on the same layer or on the top layer to produce multiple resonant frequencies that results in a wider bandwidth [3], [21], [22] by applying ten parasitic patches. In particular, we show that by applying the 10 PPs per element, the 2×2 sub-array attains a bandwidth of 730 MHz, 163 MHz wider than that of the two-element sub-array with five parasitic patch elements reported before [20], or a fractional bandwidth enhancement of 29%. With the 10 PPs, the element dimension becomes larger, increasing the length by 3%, the width by 41% and the overall size of the dimension area by 45% compared to [19]. This enforces the use of larger element spacing, in this case 0.75λ, thereby reducing the mutual coupling down to below −20 dB. However, this yields an insignificant grating lobe effect since the main beam is directed to the front. As a result, the proposed sub-array antenna is suitable for use in M-MIMO 5G applications. Our contribution here is in the use of a much larger number of parasitic patches, i.e., ten of those, for each element, whereas in the literature only a maximum of 4 or 5 PPs per element have been tried. The slight increase in the element dimension is paid off by the increase in bandwidth from around 600 MHz to over 700 MHz.

The 2×2 sub-array antenna design for the M-MIMO antenna system is optimized for minimum mutual coupling. The design method is first carried out by the use of a rectangular patch antenna (RMPA) design of a single element without parasitic patches. Second, the single element with 5 PPs is realized [20]. Third, another single element with the addition of 10 PPs is designed and realized in this paper. Finally, 2×2 sub-arrays of elements with 5 PPs each and 10 PPs with spacing of 0.75λ are realized and analyzed for bandwidth and mutual coupling.

This paper is structured as follows. Section II describes the antenna design, Section III reports the evaluation of the mutual coupling effect of the 2×2 sub-array antennas, and Section IV gives the conclusions.

II. ANTENNA DESIGN

The microstrip antenna design starts with identifying the appropriate specifications based on the needs of 5G applications. 5G bandwidth requirement at 3.5 GHz is 500 MHz, according to ETSI [23]. The antenna is rectangular in shape with PPs to increase the bandwidth. The designs include elements of 5-PP type, i.e., a rectangular patch with five parasitic patches, and those of 10-PP type, which involve ten parasitic patches. The structure consists of a patch, a dielectric substrate and a ground layer. The media used herein are of FR-4 (epoxy) type with a dielectric constant (ε_r) of 4.3 and a substrate thickness (h) of 1.6 mm. The main patch is fed with a coaxial probe. Expected specification parameters are a bandwidth of more than 500 MHz, a return loss (RL) of less than −10 dB, a mutual coupling of less than −20 dB, and a frequency of 3.5 GHz.

The rectangular antenna design process involves mathematical calculation for the width and length of the patch, substrate, and ground and determining the coordinates of the coaxial probe [24], [25]. The dimensional design of the parasitic patch also uses the same mathematical equations as the rectangular patch. The parasitic patch technique is applied by adding a parasitic patch in the E-plane and H-plane [3]. The dimensions of a single element without and with PPs

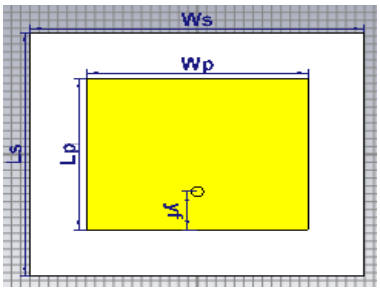

FIGURE 1. Single element (SE).

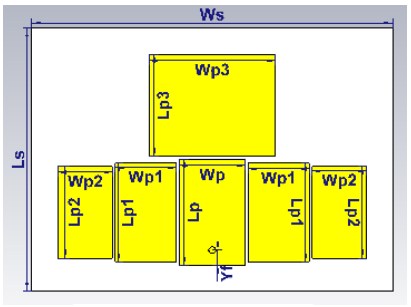

Dimension D1(mm)

W_s	66.71	W_{p1}	11.31
L_s	48.58	L_{p1}	18.27
W_p	12.25	W_{p2}	10.12
L_p	19.59	L_{p2}	16.97
X_f	6.09	W_{p3}	23.39
Y_f	2.8	L_{p3}	18.89

FIGURE 2. The 5-PP element.

are displayed using CST software. Figs. 1, 2 and 3 show the resulting dimensions.

A. SINGLE ELEMENT ANTENNA

Herein we use a single rectangular element (SE) to refer to one that does not include any parasitic patch. The dimensions of the SE can be seen in Fig. 1, the design of which follows the method in [24]. The element size is $W_s = 35.93$ mm, $L_s = 30.86$ mm, $W_p = 23.75$ mm, $L_p = 19.19$ mm, $Y_f = 4.87$ mm. Hence, the size is 35.93 mm $\times$ 30.86 mm ($0.42\lambda \times 0.36\lambda$).

B. 5-PP ELEMENT

The dimensions of the single element with 5 PPs can be seen in Fig. 2 and has been described in [20]. The element size of 5 PPs is 66.71 mm $\times$ 48.58 mm ($0.78\lambda \times 0.36\lambda$).

C. 10-PP ELEMENT

The dimensions of a single element with 10 PPs can be seen in Fig. 3. The element size of 10 PPs is 68.71 mm $\times$ 68.48 mm ($0.80\lambda \times 0.79\lambda$). The element with 10 PPs is developed from the element with 5 PPs by adding five parasitic patches. In the new element, several changes are made to the parasitic patches, especially in the dimensions *Wp* and *Lp*, *Wp*1 and *Lp*1, *Wp*2 and *Lp*2, *Wp*3 and *Lp*3, as well as the addition of parasitic patches with dimensions *Wp*4 and *Lp*4, *Wp*5 and *Lp*5, *Wp*6 and *Lp*6. The length and width of the parasitic patch as well as the placement of the parasitic patch horizontally

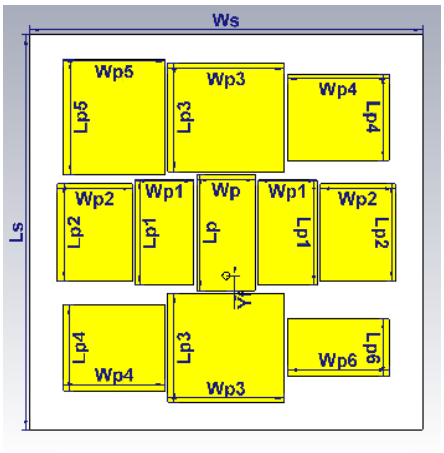

Dimension D2 (mm)

W_s	68.71	W_{p1}	10.31	W_{p4}	17.77
L_s	68.49	L_{p1}	18.27	L_{p4}	15
W_p	10.25	W_{p2}	13.12	W_{p5}	17.77
L_p	20.11	L_{p2}	16.97	L_{p5}	20
X_f	6.09	W_{p3}	20.39	W_{p6}	17.77
Y_f	2.8	L_{p3}	10.31	L_{p6}	10

FIGURE 3. The 10-PP element.

(right and left) and vertically (up and down) determine the new resonant frequency, which increases the bandwidth [3]. The positions of parasitic patches with dimensions *Wp*4 and *Lp*4, *Wp*5 and *Lp*5, *Wp*6 and *Lp*6 are as shown in Figure 3. The parasitic patches obtain electric current due to induction from those with dimensions *Wp* and *Lp*. When the patch of dimensions *Wp* and *Lp* is supplied with electric current, it causes induction on the radiating side of the parasitic patch. Due to the proximity of the parasitic patches to each other, the parasitic patch on the non-radiating side generates an electric current induced from the parasitic patch on the radiating side.

D. 2 $\times$ 2 SUB-ARRAY

This paper reports on two sub-array antenna designs, each consisting of 5-PP and 10-PP elements. The 2 $\times$ 2 sub-arrays are simulated to evaluate the effect of mutual coupling with element spacings, defined herein as spacings between adjacent points of element feeding, of 0.75λ or 64.28 mm. The dimension of the 2 $\times$ 2 sub-array composed of 5-PP elements is 130.99 mm $\times$ 112.86 mm ($1.53\lambda \times 1.32\lambda$), while the one for the sub-array consisting of 10-PP elements is 132.99 mm $\times$ 132.77 mm ($1.55\lambda \times 1.54\lambda$). The design of the 2 $\times$ 2 sub-arrays can be seen in Fig. 4.

III. EVALUATION OF MUTUAL COUPLING EFFECT

A. SURFACE CURRENT PERFORMANCE

Figs. 5(a) and (b) demonstrate the distribution of surface currents over the 2 $\times$ 2 sub-arrays with 5-PP and 10-PP elements. A significant spacing of 0.75λ between adjacent antenna elements reduces the surface current crossing over the elements the 2 $\times$ 2 subarray. It should be noted that for this application the grating lobe is not a problem because the main lobe points forward so that the grating lobe points to

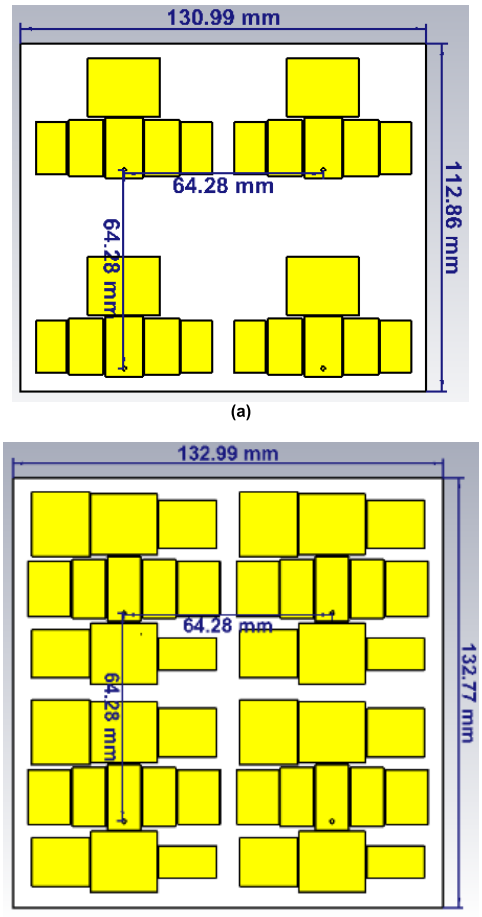

FIGURE 4. Designs of 2 × 2 sub-arrays with elements of type: (a) 5-PP (b) 10-PP.

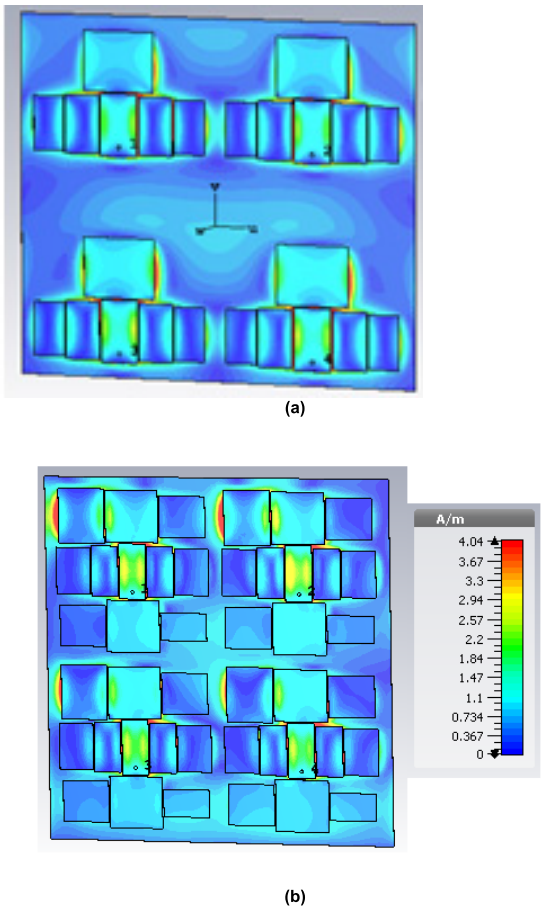

FIGURE 5. Surface current distribution of 2 × 2 sub-array antenna with elements composed of (a) 5 PPs dan (b) 10 PPs.

TABLE 1. Comparison of simulation and measurement results for elements of type SE, 5-PP and 10-PP.

Parameter	SE		5 PPs		10 PPs	
	Sim.	Meas.	Sim.	Meas.	Sim.	Meas.
B (MHz)	139	115	618	550	732	722
FB (%)	3.97	3.22	17.04	14,8	20.5	19.83
RL (S11)	−34.86	−19.74	−11.45	−20.21	−14.03	−18.42

the back and is of small value because the spacing between elements is 0.75 λ(less than λ).

Meanwhile, the presence of parasitic patches in the 5-PP and 10-PP elements suppresses even further the surface currents across the 2 × 2 subarray.

B. SCATTERING PARAMETER PERFORMANCE

Fig. 6 shows the modeling results as well as measurements of RL, measured in S11, and bandwidth of single elements of 5 PPs and 10 PPs. The simulation results of a single element without PPs show that the bandwidth is 139 MHz, the fractional bandwidth is 3.97% and the RL at 3.5 GHz is −34.86 dB, whereas for the single element with 5 PPs the bandwidth is found to be 618 MHz, the fractional bandwidth 17.04% and the RL −11.45 dB at 3.5 GHz. For the single-element antenna with 10 PPS the bandwidth is 732 MHz or 20.5%, while the RL at 3.5 GHz is −14.03 dB.

Measurement results for a single element without parasitic patches show a bandwidth of 115 MHz, a fractional bandwidth of 3.22% and RL at 3.5 GHz of −19.74 dB. For a single element having 5 PPs, the bandwidth is 550 MHz or 14.8%, and the RL at 3.5 GHz is −20.21 dB, whereas for an element with 10 PPs the bandwidth becomes 722 MHz, the fractional bandwidth becomes 19.83% and the RL at 3.5 GHz is −18.42 dB.

Fig. 6 shows that the RL measurements for elements with 5 PPs and 10 PPs are better than the simulation results. However, the RL from the SE simulation has a better result than the measurement. Meanwhile, the measured bandwidth is narrower than the simulation result. The difference between the measurement and simulation results is caused by imperfections in fabrication and measurement of the antennas. Simulation and measurement results have differences in magnitude but behave similarly and show a wider bandwidth than the original type, which is a single element without parasitic.

Comparison of simulation and measurement results of SE, 5-PP and 10-PP elements at 3.5 GHz in terms of performance parameters of a single element design are shown in Table 1. For the 5-PP elements, the simulation results are

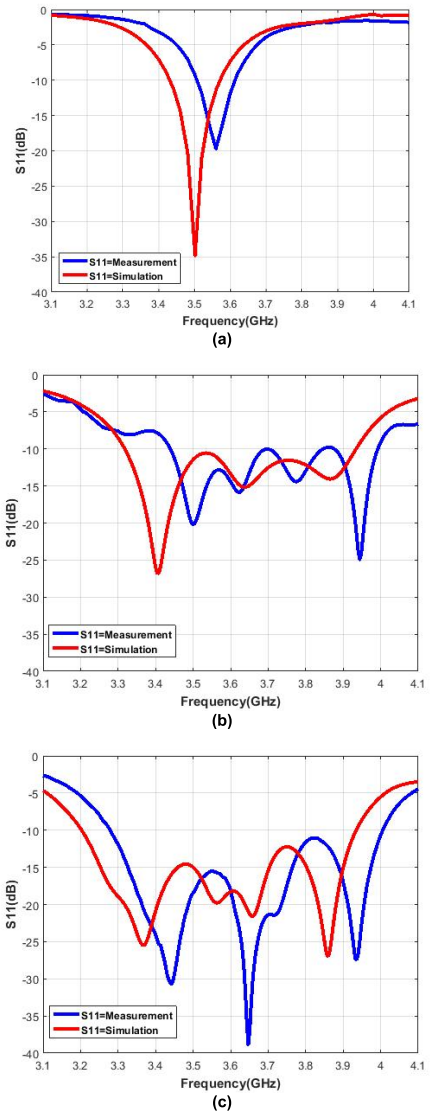

FIGURE 6. Return loss and bandwidth simulation results for elements of type: (a) SE (b) 5-PP and (c) 10-PP.

taken from [20], while the measurement is made by these authors. The parameters include bandwidth (B), fractional bandwidth (FB) and RL. The simulation results of SE show a bandwidth of 139 MHz, whereas the 5-PP exhibits a bandwidth of 618 MHz, an increase of 479 MHz from SE. Furthermore, the 10-PP with even more parasitic patches shows a bandwidth of 732 MHz, increasing by 114 MHz from the 5-PP and by 593 MHz from SE, so that the fractional bandwidth becomes 20.5%. Similarly, from the measurement results, SE only exhibits a bandwidth of 115 MHz, while the 5-PP element has a wider bandwidth of 550 MHz, also an increase of 435 MHz over SE. The 10-PP has an even broader bandwidth of 722 MHz, 172 MHz more than the 5-PP and 607 MHz more than the SE, with a fractional bandwidth of 19.83%. Hence, the 10-PP at 3.5 GHz produces the widest bandwidth to accommodate the requirements of 5G applications.

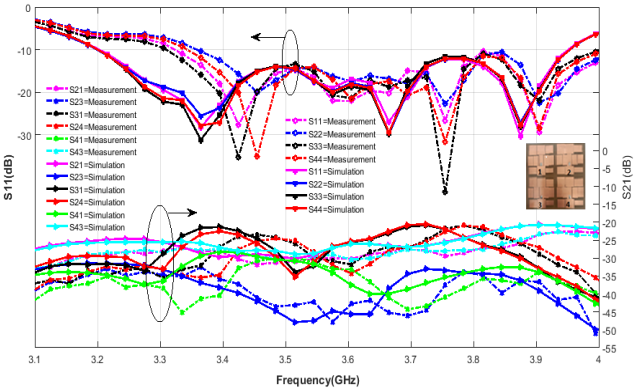

FIGURE 7. The comparison of simulation and measurements of S-parameters 2 × 2 subarray of 10 PPs elements.

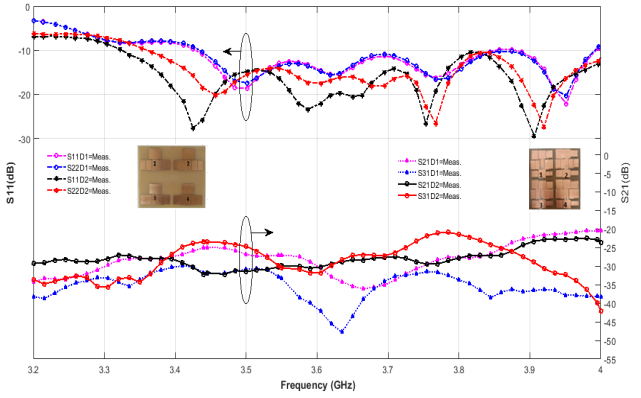

FIGURE 8. The comparison of measurements of S -parameters 2 × 2 subarray of 5 PPs and 10 PPs elements.

As a follow-up, simulations and measurements of the 2 × 2 sub-arrays with 5-PP and 10-PP elements are made to evaluate the effect of mutual coupling, because these two element types fulfill the desired 5G requirements in terms of wide bandwidth. The results for 2 × 2 sub-array of the 10-PP elements are shown in Fig. 7 and recapitulated in Table 2. They show that the sub-array meets the desired RL performance, which is less than −10 dB. There is a shift in the working frequency range of the measured sub-array with respect to the simulated design, but the range still includes the desired 3.5 GHz band required for 5G applications.

Simulation and measurement results of mutual coupling effects in the 2 × 2 sub-array of 10 PPs elements are in accordance with the desired mutual coupling performance, which is less than −20 dB. The mutual coupling at 3.5 GHz, indicated by S21, S23, S24, S31, S41, and S43, are shown in Table 2. It is clear that mutual coupling for all 2 × 2 sub-array designs observed from simulations and measurements at 3.5 GHz already meets the desired performance parameters.

Fig. 8 compares measurements of the s-parameters of the 2 × 2 subarray antenna of 5-PP and 10-PP elements. The results of measurements of RL for all elements, i.e., S11, S22, S33, and S44 at 3.5 GHz, show that the sub-array achieves the desired RL performance of less than −10 dB, which is given in Table 2. The results for mutual coupling also meet

TABLE 2. Comparison of simulation results and measurements of 2 × 2 sub-array.

Parameter	5 PPs		10 PPs	
	Sim.	Meas.	Sim.	Meas.
B (MHz)	607.8	567	745.9	730
FB (%)	16.75	15.27	20.85	19.83
S11	−18.60	−11.39	−14.03	−14.77
S22	−17.40	−11.39	−14.07	−15.45
S33	−18.72	−11.91	−13.84	−13.67
S44	−17.65	−11.91	−13.93	−15.79
S21	−29.06	−26.79	−29.89	−33.01
S23	−38.42	−32.66	−46.25	−31.11
S31	−37.73	−28.20	−30.34	−24.71
S24	−37.73	−30.88	−32.31	−29.63
S41	−38.42	−30.16	−32.62	−31.62
S43	−32.22	−27.84	−28.39	−35.11

the desired performance, which is less than −20 dB. The measured mutual coupling at 3.5 GHz, namely S21, S23, S24, S31, S41, and S43 are also shown in Table 2.

The mutual coupling effect depends also on the relative positions of the elements in the antenna array. Suppose the antenna array elements are spaced too close together, then significant mutual coupling can cause a decrease in efficiency and change the radiation pattern. On the other hand, if the elements are too far apart, the substrate dimensions increase and the efficiency decreases. The effective or minimum spacing between elements that are safe from the effect of mutual coupling is 0.5λ [24]. In this sub-array design, the element spacing is 0.75λ and, therefore, the mutual coupling is suppressed.

The return losses from measurement indicated by S11, S22, S33 and S44 for the 2 × 2 sub-array of 5-PP elements are consistently smaller than the corresponding losses for the 2 × 2 sub-array of 10-PP elements, with the average difference being 3.27 dB. This result suggests that sub-arrays constructed from elements with fewer parasitic patches have a smaller return loss. Also from the measurement, the mutual coupling indicated by S23, S31, S24 and S41 shows a lower value with an average difference of −2.09 dB for sub-arrays of 5-PP elements relative to those of 10-PP elements. Meanwhile, the S21 and S43 measured for sub-arrays of 10-PP elements are lower than the corresponding values for those of the 5-PP elements, with an average difference of −4.98 dB. However, in general it can be concluded that the 2 × 2 sub-arrays of 10-PP elements, each having ten parasitic patches, demonstrate a good isolation between elements, leading to low mutual coupling. These results validate [18], [20] that the implementation of additional parasitic patches can maintain low mutual coupling. In addition, Table 2 also shows that the sub-arrays with elements having 10 PPs consistently exhibit

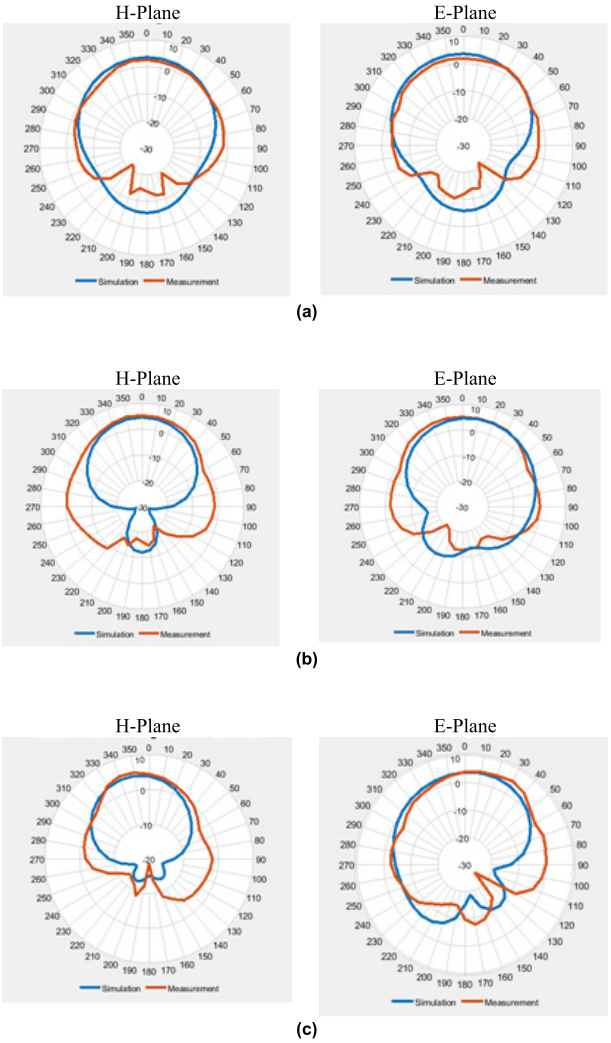

FIGURE 9. Comparison of simulation results and measurement of the radiation pattern of single antenna elements: (a) SE (b) 5 PPs-type, and (c) 10 PPs-type.

greater bandwidth than those with elements having 5 PPs. Based on the return loss for each element in Table 2, it can be safely concluded that the return loss for the overall subarray is less than −10 dB.

C. RADIATION PATTERN PERFORMANCE

Fig. 9 compares the results of simulations and measurements of radiation patterns and gains of single antennas of types (a) SE (b) 5-PP type and (c) 10-PP type. The gain shown is the maximum gain. The radiation patterns displayed are those of the H-plane (horizontal plane/azimuth) and E-plane (vertical plane/elevation). Single element gains from simulation and measurement can be seen in Table 3. The fabricated single elements of all types are each found to have gain above 2 dB.

Fig. 10 compares the simulation results and measurements of the radiation pattern and gain of the individual elements in two 2 × 2 sub-arrays having elements of type 5-PP and 10-PP, respectively. The gains for both can be seen in Table 4, in which the measured gain for both types of elements in their respective sub-arrays shows a good value. The radiation

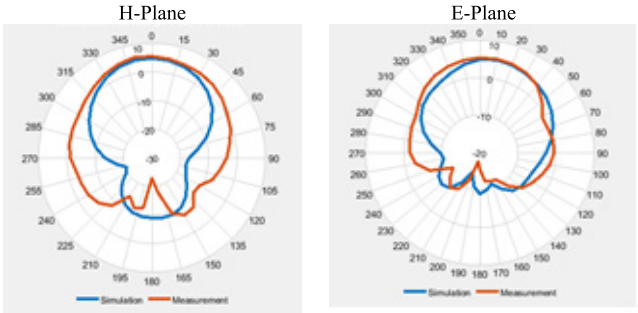

(a)

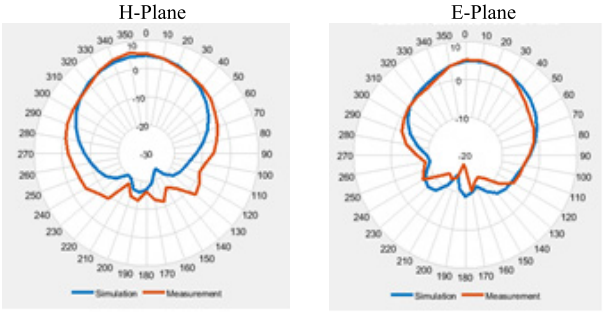

(b)

FIGURE 10. Results of simulation and measurement of radiation patterns: (a) 2 × 2 sub-array of 5 PPs elements, and (b) 2 × 2 sub-array of 10 PPs elements.

TABLE 3. Comparison of simulation and measurement results single element gain.

Single Element	Gain (dB)	
	Sim.	Meas.
SE	3.64	2.46
5 PPs-type	4.819	5.58
10 PPs-type	4.361	5.34

TABLE 4. Comparison of simulation and measurement results of element gain in 2 × 2 sub-array.

2x2 Sub-array of 5-PP elements	Gain (dB)		2x2 Sub-array of 10-PP elements	Gain (dB)	
	Sim.	Meas.		Sim.	Meas.
Element 1	5.098	5.83	Element 1	4.722	5.95
Element 2	5.089	5.48	Element 2	5.454	6.08
Element 3	5.334	5.57	Element 3	5.138	4.65
Element 4	5.334	5.23	Element 4	5.016	4.84

pattern is represented herein by that of element 1 only, while elements 2, 3 and 4 have similar patterns. The gain shown is the maximum gain.

The proposed antenna design is compared with others from the existing literature in terms of size, operating frequency, and bandwidth in Table 5. The comparison shows that the proposed antenna, a single element with 10 PPs, while being larger in size than the others, is capable to create a broader bandwidth. In the last row of Table 5 we show the size and bandwidth of the proposed 2 × 2 sub-array of elements

TABLE 5. Comparison of the performance between the proposed antenna and reference antenna.

Ref.	Antenna purpose	Antenna Size (mm^2)	Operating Frequency (GHz)	Bandwidth (MHz)
[19]	SE without parasitic patch	32.60 x 24.05	2.8	88.2
[18]	SE with four parasitic patches	62 x 62	3.3 - 3.91	610
[18]	2x2 array with four parasitic patches	160 × 160	3.38 - 3.95	570
[20]	SE with five parasitic patches	66.71 x 48.58	3.5	618
Proposed antenna	10-PP type element	68.71 x 68.48	3.5	732
Proposed antenna	2x2 sub-array of 10-PP type elements	132.99 x 132.77	3.5	730

with 10 PPs each, which is smaller and provides a wider bandwidth than the array in [18].

IV. CONCLUSION

The single element with 10 PPs shows a broader bandwidth of 722 MHz, which is equivalent to a fractional bandwidth of around 20%, an increase of 172 MHz from that of the five-parasitic patch element and a larger increase of 607 MHz from that of single element without parasitic patches. It can be concluded that the addition of parasitic patches can enhance the bandwidth. It turns out that the bandwidth improvement is also observed for the 2 × 2 sub-arrays employing elements with ten PPs relative to the sub-arrays of elements with five parasitic patches, i.e. increasing the bandwidth by as much as 163 MHz or 29%.

The results of simulation and measurement for the 2 × 2 sub-arrays of elements with 5 and 10 PPs at 3.5 GHz show that both sub-arrays meet the desired performance because the return loss is less than −10 dB for both. Comparison of simulation results and measurement of mutual coupling of the two 2 × 2 sub-arrays are also in agreement with the desired performance, i.e., less than −20 dB. Therefore, generally the increase in the number of parasitic patches added to each element yields the same order of mutual coupling in the sub-array, while successfully improving the bandwidth. In overall, the antenna meets the desired specifications and is applicable as a 5G communication antenna.

REFERENCES

[1] E. G. Larsson, O. Edfors, F. Tufvesson, and T. L. Marzetta, "Massive MIMO for next generation wireless systems," *IEEE Commun. Mag.*, vol. 52, no. 2, pp. 186–195, Feb. 2014, doi: 10.1109/MCOM.2014.6736761.

[2] L. Lu, G. Y. Li, A. L. Swindlehurst, A. Ashikhmin, and R. Zhang, "An overview of massive MIMO: Benefits and challenges," *IEEE J. Sel. Topics Signal Process.*, vol. 8, no. 5, pp. 742–758, Jun. 2014, doi: 10.1109/JSTSP.2014.2317671.

[3] S. A. R. Parizi, "Bandwidth enhancement techniques," in *Microstrip Antennas: Trends in Research*, vol. 1, 2017, doi: 10.5772/intechopen.70173.

[4] P. N. Fletcher, M. Dean, and A. R. Nix, "Mutual coupling in multi-element array antennas and its influence on MIMO channel capacity," *Electron. Lett.*, vol. 39, no. 4, pp. 342–344, Feb. 2003, doi: 10.1049/el:20030219.

[5] X. Chen, S. Zhang, and Q. Li, "A review of mutual coupling in MIMO systems," *IEEE Access*, vol. 6, pp. 24706–24719, 2018, doi: 10.1109/ACCESS.2018.2830653.
[6] H. Singh, H. L. Sneha, and R. M. Jha, "Mutual coupling in phased arrays: A review," *Int. J. Antennas Propag.*, vol. 2013, pp. 1–23, Mar. 2013, doi: 10.1155/2013/348123.
[7] X. Chen, S. Zhang, and A. Zhang, "On MIMO-UFMC in the presence of phase noise and antenna mutual coupling," *Radio Sci.*, vol. 52, no. 11, pp. 1386–1394, 2017, doi: 10.1002/2017RS006258.
[8] K.-H. Chen and J.-F. Kiang, "Effect of mutual coupling on the channel capacity of MIMO systems," *IEEE Trans. Veh. Technol.*, vol. 65, no. 1, pp. 398–403, Jan. 2016, doi: 10.1109/TVT.2015.2397033.
[9] M. Alibakhshikenari, M. Khalily, B. S. Virdee, C. H. See, R. Abd-Alhameed, and E. Limiti, "Mutual coupling suppression between two closely placed microstrip patches using EM-bandgap metamaterial fractal loading," *IEEE Access*, vol. 7, pp. 23606–23614, 2019, doi: 10.1109/ACCESS.2019.2899326.
[10] X. Tan, W. Wang, Y. Wu, Y. Liu, and A. A. Kishk, "Enhancing isolation in dual-band meander-line multiple antenna by employing split EBG structure," *IEEE Trans. Antennas Propag.*, vol. 67, no. 4, pp. 2769–2774, Apr. 2019, doi: 10.1109/TAP.2019.2897489.
[11] F. Liu, J. Guo, L. Zhao, X. Shen, and Y. Yin, "A meta-surface decoupling method for two linear polarized antenna array in sub-6 GHz base station applications," *IEEE Access*, vol. 7, pp. 2759–2768, 2019, doi: 10.1109/ACCESS.2018.2886641.
[12] H. Qi, L. Liu, X. Yin, H. Zhao, and W. J. Kulesza, "Mutual coupling suppression between two closely spaced microstrip antennas with an asymmetrical coplanar strip wall," *IEEE Antennas Wireless Propag. Lett.*, vol. 15, pp. 191–194, 2016, doi: 10.1109/LAWP.2015.2437995.
[13] Y. Gao, R. Ma, Y. Wang, Q. Zhang, and C. Parini, "Stacked patch antenna with dual-polarization and low mutual coupling for massive MIMO," *IEEE Trans. Antennas Propag.*, vol. 64, no. 10, pp. 4544–4549, Oct. 2016, doi: 10.1109/TAP.2016.2593869.
[14] Z. Niu, H. Zhang, Q. Chen, and T. Zhong, "Isolation enhancement for 1×3 closely spaced e-plane patch antenna array using defect ground structure and metal-vias," *IEEE Access*, vol. 7, pp. 119375–119383, 2019, doi: 10.1109/ACCESS.2019.2937385.
[15] K. S. Vishvaksenan, K. Mithra, R. Kalaiarasan, and K. S. Raj, "Mutual coupling reduction in microstrip patch antenna arrays using parallel coupled-line resonators," *IEEE Antennas Wireless Propag. Lett.*, vol. 16, pp. 2146–2149, 2017, doi: 10.1109/LAWP.2017.2700521.
[16] M. G. Alsath, M. Kanagasabai, and B. Balasubramanian, "Implementation of slotted meander-line resonators for isolation enhancement in microstrip patch antenna arrays," *IEEE Antennas Wireless Propag. Lett.*, vol. 12, pp. 15–18, 2013, doi: 10.1109/LAWP.2012.2237156.
[17] N. M. Z. Iskandar, E. Setijadi, and A. Affandi, "A combination of defected ground structure and line resonator for mutual coupling reduction," in *Proc. 3rd Int. Seminar Res. Inf. Technol. Intell. Syst. (ISRITI)*, Dec. 2020, pp. 267–270, doi: 10.1109/ISRITI51436.2020.9315370.
[18] K. D. Xu, J. Zhu, S. Liao, and Q. Xue, "Wideband patch antenna using multiple parasitic patches and its array application with mutual coupling reduction," *IEEE Access*, vol. 6, pp. 42497–42506, 2018, doi: 10.1109/ACCESS.2018.2860594.
[19] F. Amillia, E. Setijadi, and G. Hendrantoro, "Subarray design with two rectangular elements for massive MIMO system development," in *Proc. Int. Conf. Adv. Mechatronics, Intell. Manuf. Ind. Autom. (ICAMIMIA)*, Oct. 2019, pp. 1–6.
[20] A. R. Pratiwi, E. Setijadi, and G. Hendrantoro, "Design of two-elements subarray with parasitic patch for 5G application," in *Proc. Int. Seminar Intell. Technol. Its Appl., Hum. Reliab. Intell. Syst. (ISITIA)*, Jul. 2020, pp. 311–316, doi: 10.1109/ISITIA49792.2020.9163785.
[21] K. Ding, C. Gao, B. Zhang, Y. Wu, and D. Qu, "A compact printed unidirectional broadband antenna with parasitic patch," *IEEE Antennas Wireless Propag. Lett.*, vol. 16, pp. 2341–2344, 2017, doi: 10.1109/LAWP.2017.2718000.
[22] K. D. Xu, H. Xu, Y. Liu, J. Li, and Q. H. Liu, "Microstrip patch antennas with multiple parasitic patches and shorting vias for bandwidth enhancement," *IEEE Access*, vol. 6, pp. 11624–11633, 2018, doi: 10.1109/ACCESS.2018.2794962.
[23] *5G; NR; User Equipment (UE) Conformance Specificatio; Radio Transmission and Reception; Part 2: Range 2 Standalone (3GPP TS 38.521-2 Version 15.3.0 Release 15)*, document 3GPP TS 38.101-1, TS 138 521-2, Version 15.2.0, 15.3.0, Release 15, ETSI, 2018, pp. 1–72. [Online]. Available: https://portal.etsi.org/TB/ETSIDeliverableStatus.aspx
[24] C. A. Balanis, *Antenna Theory: Analysis and Design*, 4th ed. Hoboken, NJ, USA: Wiley, 2016.
[25] A. Majumder, "Rectangular microstrip patch antenna using coaxial probe feeding technique to operate in S-band," *Int. J. Eng. Trends Technol.*, vol. 4, pp. 1206–1210, Apr. 2013. [Online]. Available: http://www.ijettjournal.org/volume-4/issue-4/IJETT-V4I4P340.pdf.

FITRI AMILLIA (Student Member, IEEE) was born in Blitar, Indonesia, in August 1977. She received the B.Eng. degree in electrical engineering from the Universitas Muhammadiyah of Malang (UMM), Indonesia, in 2001, and the M.Eng. degree in electrical engineering from the Institut Teknologi Sepuluh Nopember (ITS), Surabaya, Indonesia, in 2006, where she is currently pursuing the Ph.D. degree in electrical engineering. She is also working as a Senior Lecturer with the Universitas Islam Negeri Sultan Syarif Kasim Riau, Pekanbaru, Indonesia. Her research interests include multi-antenna wireless communications, microstrip antenna design, as well as phased array and massive MIMO.

EKO SETIJADI (Member, IEEE) was born in Indonesia, in October 1972. He received the B.Eng. and M.Eng. degrees in electrical engineering from the Institut Teknologi Sepuluh Nopember (ITS), Surabaya, Indonesia, and the Ph.D. degree in electrical engineering from Kumamoto University, Japan. He is currently an Associate Professor with the Department of Electrical Engineering, ITS. His current research interests include antenna design, microwave circuits, and metamaterials, including metasurface for communication and radar applications, electromagnetic compatibility, communication network design and optimization, and engineering education.

GAMANTYO HENDRANTORO (Senior Member, IEEE) was born in Jombang, Indonesia, in November 1970. He received the B.Eng. degree in electrical engineering from the Institut Teknologi Sepuluh Nopember (ITS), Surabaya, Indonesia, in 1992, and the M.Eng. and Ph.D. degrees in electrical engineering from Carleton University, Ottawa, ON, Canada, in 1997 and 2001, respectively. He is currently a Professor with the Department of Electrical Engineering, ITS. He has been involved in various studies, including investigation into millimeter-wave propagation, radio channel modeling and wireless systems for tropical areas, studies on HF skywave channels and communications in equatorial regions, and development of radar array and signal processing. His current research interests include radio propagation channel modeling and wireless communications.